06

Influence of FeS nanoinclusions on photoelectric characteristics of CdS:Fe

© S.V. Stetsyura, P.G. Kharitonova, A.M. Zakharevich

Saratov State University,
410012 Saratov, Russia
e-mail: haritonovapg@gmail.com

Received January 2, 2025
Revised January 2, 2025
Accepted January 2, 2025

We modified the surface of single-crystal CdS using an organic coating of iron arachinate obtained by the Langmuir-Blodgett technology, followed by annealing of the resulting hybrid structure. We have demonstrated the possibility of forming a heterophase structure of the diluted magnetic semiconductor CdS-FeS, which has an extended range of properties. We carried out a study of the chemical composition before and after modification of the CdS surface by an organic coating. Variation the number of deposited iron arachinate monolayers made it possible to change the parameters of the limited iron source within the required limits, ensuring the formation of ferromagnetic phase nanoinclusions of size-defined at a target depth. The prediction of the size of the FeS phase and its distribution by depth was carried out by modeling the simultaneous processes of Fe diffusion, formation and precipitation of nanosized inclusions of the magnetic phase. We have determined the optimal number of monolayers in the coating (25−35), which ensures the formation of precipitates larger than 3 nm at a depth of at least 0.21 μm, and an increase in the photosensitivity of the obtained material by 20−40 times.

Keywords: heterophase material, nanoscale precipitates, photosensitivity, Langmuir-Blodgett layers.

DOI: 10.61011/TP.2025.05.61125.471-24

Introduction

The diluted magnetic semiconductors (DMS), or semimagnetic semiconductors, represent the new class of magnetic materials in terms of their properties between the ferromagnetic and semiconductors [1]. DMS is obtained from non-magnetic semiconductors by doping them with magnetic elements, which leads to a unique combination of magnetic and optical properties of these materials. Molecular beam epitaxy methods are successfully used for fabrication of DMS which can be used to form both, thin DMS films and multilayer DMS heterostructures [2]. As the basis of DMS the compound-semiconductors are widely used, e.g. III-V (GaAs, InAs), II-VI (CdTe, ZnO, ZnS, ZnTe), IV-VI (TiO_2 SnO_2) and/or elements of IV group (Si, Sn, Ge) doped with transition metals (Sc, Fe, Mn, Co, Ti, Cr, Ni, Cu) [3]. Currently, the DMS with compound-semiconductors A2B4 and A3B5, doped with atoms (ions) of transition metals such as V, Cr, Mn, Fe, Co, Ni are of high interest to the researchers [4]. Such DMS are perspective candidates for use in magnetooptical devices [5–7], nonvolatile memory [8], biosensors, as well as spintronic devices [9,10].

Among the semiconductors of A2B6 type there's cadmium sulfide (CdS) that has quite large width of the band gap (2.42 eV) and is widely used in various optoelectronic and photovoltaic applications [11]. By doping CdS with such magnetic elements as Mn, Fe and Co [12] it is possible to obtain DMS both, as solid solutions and as heterophase structures on its basis. In recent 15−20 years much of the research has been carried for CdS doped with Fe. These studies were aimed at obtaining CdS-FeS heterostructures using various technologies, as well as at characterizing their properties [13] and searching for areas of effective application.

One of the most interesting examples of using CdS-FeS nanocomposites is given in paper [14], the authors of which showed that inclusion of CdS-FeS nanocomposites in the organic biosensitive matrix based on poly(o-)phenylenediamines improved the biosensor's amperometric response, which allowed to use the new material for detecting E. coli bacteria.

Depending on the technologies used, the authors were able to obtain both, solid solutions $Cd_xFe_{1-x}S$ and nanocomposites CdS-FeS [15] with various ferromagnetic, optical, and photoelectric properties. Since Fe doping should lead to occurrence of magnetic properties, these properties were usually studied first [16]. Magnetic properties of the obtained DMS are also described in [13,17].

Quite a lot of publications have also been devoted to changing optical properties when creating DMS using various technologies [18–22]. For example, in paper [18], it was experimentally shown that iron doping of CdS thin films by ion implantation reduces the optical band gap from 2.39 to 2.17 eV with an increase in Fe concentration in a certain concentration range without occurrence of secondary phases and Fe precipitates, but with a significant lattice disordering. The authors [19] fabricated thin films of CdS:Fe with various concentrations of dopants (0, 0.1, 0.2 and 0.3 wt.%) on a glass substrate using modified instantaneous evaporation

system. Based on the results of recorded photoluminescence spectra, they found that the photoluminescence intensity of CdS:Fe film increases with the rise of iron concentration. In the framework of a study in [20], the optical properties of Fe-doped thin films of CdS produced using electron beam evaporation technology under the influence of gamma radiation are discussed. The authors have shown that CdS:Fe samples with different concentrations of dopant are affected by gamma radiation, the effect of which leads to an enlarged optical band gap. In paper [21], researchers propose to use the electrodeposition method to fabricate polycrystalline thin films CdS:Fe on SnO_2 substrate. The authors have shown the applicability of this method for obtaining CdS:Fe, but it was noted that the films were significantly disordered and the density of dislocations in the material increased 1.5 times even at 2 at.% of interstitial Fe. In [22] it is shown that CdS:Fe nanomaterials can be effectively used as a filler for a polymer mix matrix. This paper describes the preparation and optical parameters of a polymer mixture with the addition of CdS:Fe nanophase in the amount of 1, 3, 5 and 10 mass%. Based on the results of measurements of optical parameters, the authors found that refractive index of the studied polymer mixture increased from 1.05 to 1.19 with the addition of 10 % CdS:Fe synthesized in the air or up to 1.2 with the addition of the same amount of CdS:Fe synthesized in the presence of N_2. At the same time, the fluorescence intensity of the polymer mixture increased with the addition of only 3 % CdS:Fe obtained in the air.

Despite the fact that CdS is a very photosensitive material in the visible region of spectrum, the photoelectric characteristics of CdS:Fe material received almost no attention. Nevertheless, the results available in this area indicate the prospects for their study. Thus, in the study [23], Fe-doped CdS thin films were synthesized using spray pyrolysis, and by measuring resistance in the dark and under illumination, the authors showed that Fe dopants with a certain concentration acted as centers of quenching of CdS photoconductivity, and with a large fraction of FeS phase the photosensitivity of the material in the wavelength range of 300–800 nm almost completely disappeared. Since photosensitivity was maintained and performance increased at low concentrations of Fe as a dopant, the authors of [23] suggested that CdS:Fe film structures may be used in optical sensors that require a fast response and return to normal when illumination is turned off. It should be noted that the authors used compositions with only a high percentage of FeS (from 5 to 20 at.%), recorded the heterophase composition of films using X-ray diffraction analysis, but neglected it when analyzing the photovoltaic characteristics.

Earlier we emphasized [24], that it is possible to obtain DMS on the basis of CdS, having used Fe coatings for doping through Langmuir-Blodgett (LB) technology. This technology provides high accuracy of dosing the dopant [25] and produces the nanoinclusions of FeS phase in matrix of solid solution $Cd_xFe_{1-x}S$. Using standard model of dopant diffusion from a limited source, taking into account the FeS precipitation processes occurring due to the limited solubility of CdS and FeS components, it is possible to optimize the phase composition of the CdS-FeS material, which will exhibit magnetic properties and maintain maximum photosensitivity in the visible region of the spectrum.

Thus, in this work, the focus will be on modeling the phase composition of CdS-FeS material obtained using LB technology and studying the changes in photosensitivity of CdS during the formation of nanostructured material CdS-FeS.

1. Materials, technologies and methods of composition characterization

1.1. Description of materials and technologies used

In the present work, samples of monocrystalline CdS with an iron-containing coating based on organic matrix were obtained and studied. The coating consisted of one or more iron arachinate (ArchFe) monolayers obtained using LB technology and placed on CdS surface using Langmuir-Schaeffer method. When CdS substrate moves from top to bottom, *X*-type layers are formed. When the hydrophilicity or hydrophobicity of the substrate is not strongly expressed, the layer transfer in this way occurs with a coefficient close to unity, i.e. the area of the substrate is almost completely covered by the transferred layer.

The organic films doped with iron were obtained on system KSV-Nima LB Through Medium KN 2002 (KSV-Nima, Finland). $FeCl_3$ (produced by Sigma Aldrich, chemically pure) with a concentration 10^{-3} mol/l in water solution was used as a source of iron. To obtain monolayers, arachic acid (produced by Sigma Aldrich) was diluted in chloroform to a concentration of 10^{-3} mol/l and 50 μl of this volume was injected onto the surface of an aqueous solution of $FeCl_3$ with a pH of 4.20 ± 0.05. The indicated concentrations, amount, and pH of arachic acid solution and aqueous solution of $FeCl_3$ ensured the formation of a tightly packed monolayer of ArchFe on the surface of the aqueous subphase, as previously shown by us in [24]. Next, the monolayers were compressed at a rate of 25 mm/min until a tightly packed layer was formed. The transfer of iron-containing monolayers to a solid substrate was carried out while maintaining a set surface pressure. The value of the surface pressure was estimated based on the analysis of π-A isotherms and amounted to 17 mN/m. To increase the surface density of Fe on CdS surface, several batches of samples with different numbers of monolayers in the coating were obtained: 1, 5, 10, 25, 35, 45 and 50 monolayers of ArchFe. The parameters of ArchFe monolayers and the coatings obtained by their sequential application were studied and described by us in [24]. In particular, the area per molecule of ArchFe salt in the tightly packed state was determined, which was 0.32 nm^2 and the absence of Fe agglomerates attached to the film located on the surface of the aqueous subphase was demonstrated. The

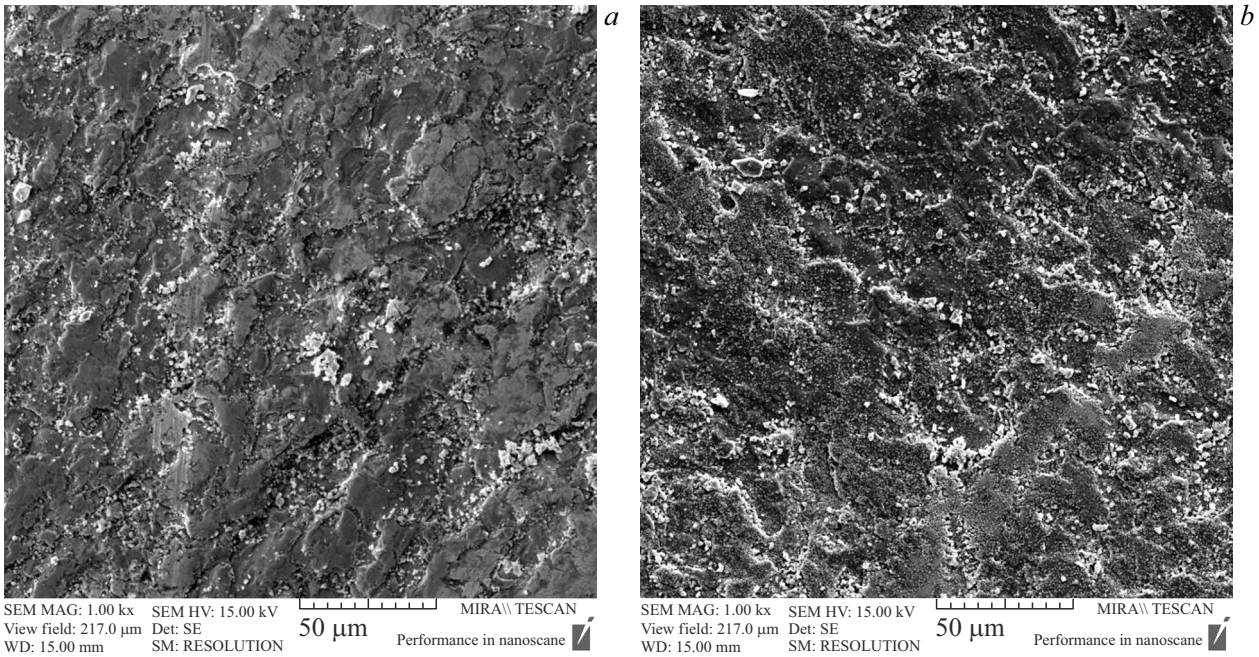

Figure 1. SEM-images of surface of CdS/ArchFe (a) and CdS:Fe (b).

area per molecule in a monolayer is a parameter that allows us to accurately determine the number of Fe atoms transferred to CdS surface and allows us to estimate the „capacity" of a limited impurity source (in our case, Fe) created using LB technology. This circumstance makes this technology unique for situations where the use of simple and inexpensive technologies makes it possible to fabricate the required limited source of dopant with high accuracy.

Further, the obtained CdS samples with ArchFe coating were annealed in the air at temperature of $(545 \pm 5)\,^{\circ}\mathrm{C}$ during 60 min. During annealing, organic matter was oxidized and decomposed to form volatile compounds and Fe atoms diffused deep into CdS to form a material conventionally designated as CdS:Fe. Atoms of Fe are known to be capable of substituting Cd atoms, however, FeS has limited solubility in CdS [26], therefore, along with paramagnetic solid solution $Cd_xFe_{1-x}S$ the ferromagnetic nano-inclusions of FeS and Fe_2O_3 phases are formed which was described in [13].

1.2. Chemical composition before and after modification of CdS surface with an organic coating

Scanning electron microscopy, energy dispersion analysis, and secondary ion mass spectrometry methods were used to characterize the chemical composition of the obtained samples and the distribution of individual chemical elements (such as iron, cadmium, sulfur, and oxygen) over the samples depth.

To determine the content of Fe in the coating on top of CdS, energy dispersion analysis (EDA) of the obtained structures was performed using autoemission scanning electron microscope MIRA 2 LMU (Tescan), equipped with the energy dispersion microanalysis system AztecLive Advanced Ultim Max 40 (Oxford Instruments Analytical Ltd., England) and software in Russian. Studies before and after high-temperature annealing were carried out by scanning at least 3 sites with an area of $217 \times 217\,\mu\mathrm{m}^2$ for each sample at an accelerating primary electron voltage of 15 kV, which allowed us to obtain a sufficiently high resolution. Also, due to low accelerating stress, it can be said that the chemical composition of the near-surface layer of the resulting structure has been studied. Typical images of the surface morphology measured in the secondary electron mode are shown in Fig. 1. ArchFe coating shown in Fig. 1, a consists of 25 monolayers, obtained using LB technology. Fig. 1, b shows the surface of structure CdS/ArchFe after annealing, i.e. when the organic component of coating has been evaporated and Fe has been diffused into CdS substrate. The prepared material was designated as CdS:Fe. The data on chemical composition obtained using EDA presented in Table 1 are averaged over all the studied sites and samples with ArchFe coating consisting of 25 monolayers. Table 1 shows the average values of X atomic percentages for individual chemical elements in the studied sites and the values of the standard deviation S obtained by statistical analysis for each chemical element from those indicated in the table.

Analysis of the scan data in Fig. 1, a shows that due to the small thickness of ArchFe coating, primary electrons reach CdS surface, as evidenced by a large and approximately equal proportion of Cd and S atoms that make up this chemical compound. It also follows from Table 1 that the

Table 1. Chemical composition of CdS/ArchFe structure surface before and after high-temperature annealing

Parameters of statistical distribution	O, at.%	S, at.%	Fe, at.%	Cd, at.%
X (before annealing)	25.51	37.05	4.41	33.03
S (before annealing)	4.51	1.27	0.31	3.59
X (after annealing)	42.09	18.59	0.55	38.77
S (after annealing)	2.93	3.04	0.12	0.11

values of the standard deviation characterizing the averaged compositions before annealing indicate that Fe atoms are evenly distributed in the coating over the surface of CdS substrate.

After annealing, a significant increase in the oxygen fraction is due to the oxidation of the surface during annealing with formation of Fe_2O_3 and CdO. After annealing, the percentage of Fe atoms on the surface decreased significantly (by 8 times), but the standard deviation decreased only 2.5 times, which indicates a greater heterogeneity in the distribution of Fe atoms compared to the situation before annealing. This fact proves the conclusions of our earlier [17] studies of CdS:Fe surface morphology using atomic force microscopy and phase contrast methods, which showed potential clustering of Fe atoms on CdS surface after annealing.

A significant decrease in the proportion of Fe atoms on the surface, first of all, may indicate the diffusion of iron atoms into CdS volume. To study the results of Fe diffusion in CdS, mass spectrometric studies were performed using a Perkin-Elmer mass spectrometer PHI 4300. The measurements were carried out in a dynamic mode, which made it possible to study the distribution of concentrations of various chemical elements across the depth of the sample. Argon with an accelerated ion energy of 4 keV at a beam current of 500 nA was used as the working gas for measurements. The target was sputtered at an angle of 30°. Fig. 2 shows the profiles of distribution of basic chemical elements in CdS:Fe structure after high-temperature annealing.

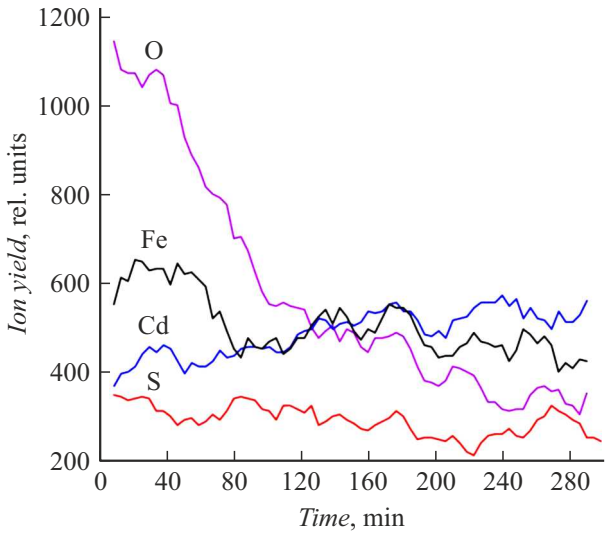

Figure 2. Profiles of distribution of chemical elements in CdS:Fe samples after high-temperature annealing of CdS doped with iron.

The etching pit obtained after mass-spectrometry was 0.9 μm. From the analysis of the dependences shown in Fig. 2, it follows that concentration of oxygen atoms decreases quite sharply with the etching depth, the sulfur profile practically does not depend on the etching depth, the amount of cadmium rises with distance from the surface from which iron diffusion occurred, and the amount of iron detected goes down accordingly. This is due to the displacement of Cd atoms from the nodes of lattice and formation of FeS. At the same time, the entire Fe profile cannot be approximated by an exponential function (which could stand for the formation of a solid solution $Cd_xFe_{1-x}S$, since the processes of Fe diffusion in CdS are going parallel with the processes of precipitation and formation of FeS at sufficiently high concentrations of Fe, which occur at short distances from the surface). Based on the depth of the etching pit and assuming the ion etching rate does not change with depth, we can estimate the depth at which precipitation processes with the formation of FeS and oxidation processes with the formation of Fe_2O_3 were particularly active. After annealing during 60 min, this depth was no more than 0.3 μm. Despite the submicron dimensions of the heterophase material layer formed as a result of the diffusion and precipitation of Fe atoms, we can talk about possible significant changes in the photovoltaic characteristics of the resulting CdS:Fe material in general, since the absorption of white light and the corresponding attenuation of the luminous flux incident on CdS plate occurs when passing through the submicron thicknesses of CdS.

Thus, in paper [27], it was shown that the addition of a narrow-band material to a wide-band photoconductive matrix leads to lower photofatigue of CdS and even to the occurrence of negative photofatigue, i.e. to a gradual increase in photocurrent during prolonged illumination of the semiconductor with constant intensity light. The model of this effect is based on the formation of a potential relief in a heterophase semiconductor, and the change in this relief under illumination, which contributes to the „drainage“ of defects into narrow-band inclusions (in this case, in FeS). As we showed earlier using the example of the heterophase material CdS-PbS [25], for effective gettering of defects under prolonged irradiation, it is sufficient to create nanoscale „drains“ in a limited volume of the sample, where incident light is actively adsorbed. However, the drains have finite „capacity“, i.e. may capture limited number of defects. At the same time, an increase in the proportion of narrow-band PbS inclusions in CdS led to a decrease in photofrequency, therefore, by analogy with the CdS-PbS material, there is a

technological problem of finding the optimal combination of the proportion of narrow-band FeS inclusions formed as a result of surface modification and annealing of CdS/ArchFe structure. Therefore, the task of modeling the processes of FeS precipitation with CdS, taking into account the limited solubility of the components, becomes an important stage in planning an experiment to create a heterophase material that exhibits high photosensitivity and has all the advantages associated with the presence of nanoscale precipitates.

2. Modeling of FeS precipitation processes in CdS, taking into account the limited solubility of the components and parameters of a limited dopant source

To describe the growth processes of FeS precipitates across the wide-band CdS matrix, we use the theory of precipitation of point defects in crystals described in [28]. In our case, iron diffusion occurs from a nanoscale coating of iron arachinate, and this layer can be considered a limited dopant source with a reflective boundary, as in the case of CdS doping from a monolayer coating of lead arachinate [29]. Since the components are only slightly soluble, during annealing, the processes of diffusion and formation of precipitates occur in parallel in the samples, which begin to grow as soon as the concentration of Fe atoms exceeds the maximum permissible concentration at a certain depth. To describe the kinetics of precipitate growth in accordance with [28], we use equation (1), since the number of particles involved in precipitation is significantly less than the total number of particles, and the effect of precipitation on the diffusion process can be neglected:

$$\frac{dN(x,t)}{dt} = -kN_C^{1-\alpha}(N(x,t)-N_E)(N_0(x,t)+mN_C - N(x,t))^{\alpha}, \quad (1)$$

where N_C — concentration of centers of precipitates nucleation, $N(x,t)$ — concentration of dopant at a depth of x from the surface after diffusion of Fe atoms throughout the annealing time t, N_E — equilibrium concentration of free iron atoms in CdS lattice, $N_0(x,t)$ — initial concentration of free Fe atoms, m — initial number of particles in the nucleation center ($m \gg 10$), k — kinetic coefficient, α — parameter found from the cluster geometry in our case is equal 0.33 provided the precipitates are having spherical shape.

The equilibrium concentration of free iron atoms N_E was found depending on the ultimate iron solubility in CdS (9 %), as a share of eigen atoms and made $1.8 \cdot 10^{17}\,\mu\text{m}^{-1}$. The centers of precipitate nucleation in our model are interstitial Cd atoms. To determine the concentration of nucleation centers N_C, an analysis of the stoichiometry of CdS single crystal was made and the proportion of excess Cd atoms located in the interstices of Cd lattice was determined, which amounted to 1.06,%. Thus, the calculated value of N_C was $6 \cdot 10^{12}\,\mu\text{m}^{-1}$ The function $N(x,t)$ is determined by solving the diffusion equation as a Gaussian function (2):

$$N(x,t) = \frac{nN_s}{\sqrt{4\pi Dt}}\exp\left(-\frac{x^2}{4Dt}\right), \quad (2)$$

where N_S — surface concentration of Fe atoms on CdS surface before annealing, D — coefficient of Fe atoms diffusion in CdS, the value of which ($D = 0.16 \cdot 10^{-10}\,\text{cm}^2/\text{s}$) was calculated via approximation of Fe profile in CdS:Fe sample (Fig. 2) using equation (2) and taking into account the diffusion time t and number of monolayers n iron arachinate. The experimental annealing time corresponding to the diffusion time t was 3600 s.

The value N_S was calculated taking into account the area per molecule of iron arachinate obtained on the basis of isotherms of monolayer compression. Average area per one molecule was $0.32\,\text{nm}^2$, which results in the value $N_S = 3.125 \cdot 10^{14}\,\text{cm}^{-2}$. The number of monolayers n ArchFe affects the parameters of the resulting coating. By changing n, you can adjust the size of FeS precipitates and control the depth of their formation. In our calculations, the number of monolayers n was selected from 1 to 50, which allowed us to determine the optimal ratio between the number of monolayers and the size of the obtained FeS inclusions.

The kinetic coefficient for substitution in equation (1) can be determined by the formula (3), considering that the limiting factor for precipitation is the rate of diffusion of atoms [28]:

$$k = 4\pi Db, \quad (3)$$

where b is the value of the order of distance between the particles in the precipitate, which is determined based on the parameters of FeS lattice.

Together, solving the equations (1) and (2) by the Runge-Kutta method of the 4th order, the values of the function of the average number of particles in the precipitate from depth (distance from the surface) and time of high-temperature treatment $< i(x,t) >$, as well as the average radius of the precipitate R were numerically found using formulae (4) and (5):

$$< i(x,t) > = \frac{1}{N_C}\int_0^t \frac{\partial N(x,t)}{\partial t}\,dt, \quad (4)$$

$$R(t) = \left(\frac{3V_0\langle i(t)\rangle}{4\pi}\right)^{1/3}, \quad (5)$$

where V_0 — volume of one molecule of FeS precipitate which is found by formula (6):

$$V_0 = \frac{M}{N_A \cdot \rho}, \quad (6)$$

where $\rho = 4.84\,\text{g/cm}^3$ — density of FeS; $M = 87.91\,\text{g/mol}$ — molar mass for FeS; N_A — Avogadro's number.

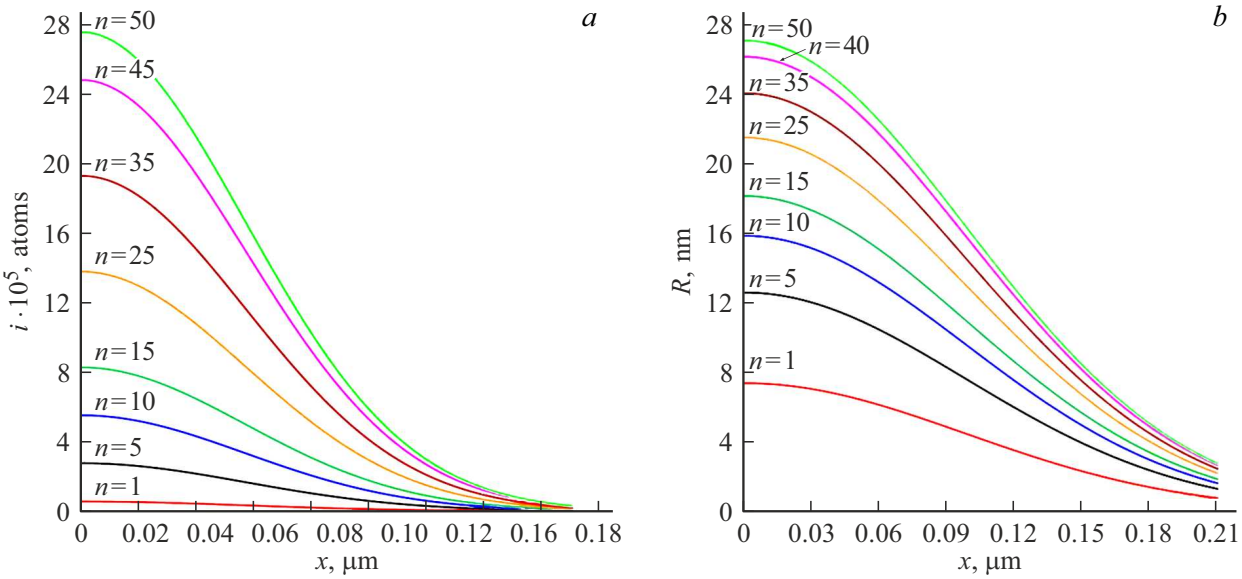

Figure 3. Calculated dependences (a) of the average number of molecules i in FeS precipitates and (b) average radius R of FeS precipitates on their burial depth x after annealing at various number n of ArchFe monolayers in the initial applied coating.

For different numbers of monolayers, the calculated dependences of the average number of particles in the precipitate (a) and its radius (b) on the depth of its occurrence are shown in Fig. 3.

The analysis of the dependences in Fig. 3 showed that precipitates are formed under the specified annealing conditions even when using a monolayer ArchFe coating as a dopant source, but the radius of the precipitates formed is significant only on the surface of CdS ($x = 0$). An rise in the number of monolayers n in the coating almost linearly increases the average number of molecules in precipitates on CdS surface, but the number n has a very weak effect on thickness of layer in which precipitation and formation of a heterophase material takes place. This is due to the fact that the limiting process in single-crystal CdS is diffusion of Fe atoms in CdS defined by annealing conditions and crystalline structure of CdS. Nevertheless, using the multi-layered ArchFe coating, it is possible to increase the average radius of FeS precipitate at a depth exceeding $0.2\,\mu$m by more than 2 times. To quantify and visualize the changes that occur with precipitates when the number of monolayers in the coating changes, we analyze the dependencies shown in Fig. 4. The maximum number of monolayers used in calculations and experiment $n = 50$, at which the average radius of FeS precipitate on the surface ($x = 0$) CdS reaches 28 nm (Fig. 4, a), and when using a monolayer source of iron the size of precipitate on the surface decreases by 4 times. The precipitation rate on the surface increases significantly when using multilayer ArchFe coatings, but in the depth of the sample, the precipitation is limited by diffusion processes, which leads to an increase in the average radius of the precipitate at a depth of only 2 times.

Fig. 4, b shows analysis of maximal distances x from the surface, where more precipitates will be recorded with an average size exceeding the set critical value (3, 5, 8 and 10 nm), depending on the multiple number of ArchFe coating layers.

The critical size of the precipitate was selected from previous experiments [25],demonstrated that the features of a heterophase photosensitive sample of CdS-type started manifesting themselves if the average size of the narrow-band precipitates of at least 3 nm was observed in a layer with a thickness corresponding to the active absorption of incident light. It was also shown that the larger the average size of the precipitates, the greater the magnitude of the effects associated with the heterophase structure. In this case, the dependence is nonlinear and there is some saturation on it. If large precipitates with a size of more than 10 nm are formed not only on the surface, but also in depth, the photosensitivity of CdS can significantly decrease due to the disordering of CdS crystal structure. Since the studies indicated in [25] were carried out on a material with a different type of narrow-band inclusions (PbS), intermediate values of critical precipitate radii (5 and 8 nm) were also used to analyze the dependencies given in this article. It follows from Fig. 4, b that with a monolayer of ArchFe coating, FeS precipitates up to 8–10 nm do not form at all, and the minimum required precipitate size of 3 nm can only be detected up to a depth of $0.14\,\mu$m. The optimal number of monolayers in the coating, according to Fig. 4, b, should be the number $n = 25 - 35$ of monolayers in the coating, which provides the formation of precipitates with a radius over 3 nm, but the proportion of precipitates reaching 10 nm is small.

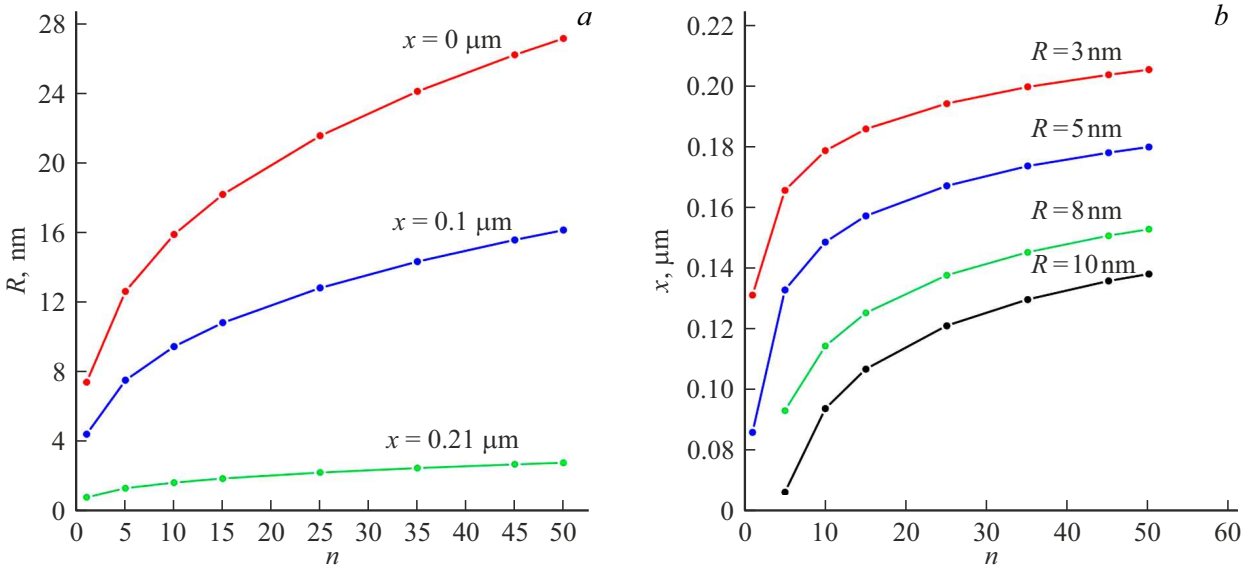

Figure 4. *a* — average radius of precipitate in the annealed structure on the surface of sample ($x = 0\,\mu$m) and in the depth of sample at a distance of 0.1 and 0.21 μm from the surface; *b* — distances from the surface of sample where precipitates with average radii of $R \geq 3$ nm, $R \geq 5$ nm, $R \geq 8$ nm and $R \geq 10$ nm are recorded depending on the number of monolayers n in the initial (before annealing) ArchFe coating.

3. Studies of FeS nanoinclusions effect on the photoelectric characteristics of CdS:Fe

CVCs were measured on the probe station PM-5 Cascade Microtech using Agilent B1500A analyzer. The presence of the probe station made it possible, without applying metal contact pads to the hybrid structures surface, to carry out measurements with precision accuracy: the distance on the surface of the studied samples (original unmodified CdS plate, hybrid CdS/ArchFe structure with a layer of ArchFe consisting of 25 monolayers, and CdS:Fe sample (obtained by annealing) between the probe contacts was kept constant and equal to 0.8 mm. A halogen lamp Matic MLK-150C was used to illuminate the samples during measurements with illumination intensity of 20 000 lx. in the surface plane of the sample. The direction of the light flux was perpendicular to the electric field lines in the studied structures during measurement of current-voltage characteristics (CVC), i.e. the mode of transverse photoconductivity was realized.

Fig. 5, *a* illustrates CVCs measured during illumination and in darkness. Due to high photosensitivity of samples and values of currents, which vary by orders of magnitude after modification of CdS composition and illumination, a semi-logarithmic scale was used. Separately, Fig. 5, *b* also shows comparison of dark currents in CdS after modification of surface with ArchFe coating and annealing of hybrid structure.

It follows from the diagram in Fig. 5, *b* that the dark current decreased 2 times after application of the organic coating, after annealing it increased slightly compared to the current in CdS/ArchFe hybrid structure, but remained less than the dark current in unmodified CdS by about 23 %. Low dark currents, all other things being equal, have a positive effect on photosensitivity of the material. However, as follows from Fig. 5, *a*, the photocurrents in the modified sample designated as CdS:Fe, also grew significantly (curve *6* in Fig. 5, *a*).

Thus, we may say about higher integral photosensitivity of the heterophaze material CdS-FeS compared to „pure“ CdS. To quantify the change in photosensitivity, we calculate the parameter k, the values of which are determined as the ratio of photocurrent at fixed values of the irradiation intensity and voltage applied to the magnitude of the dark current (Table. 2) for each of the samples.

As follows from Table 2, the change in k values is not the same for different values of U, which is due to the nonlinearity of CVCs, their different steepness at low U and the presence of current saturation region. The multiplicity k of current variation under illumination increased for heterophase CdS:Fe compared to„pure“ CdS by 20–40 times. For CdS/ArchFe hybrid structure, which in our study is an intermediate step for obtaining the heterophase CdS:Fe the growth/decline in photosensitivity varies depending on the magnitude of the applied voltage — the organic coating at low voltages limits the current and its variation in the structure impacted by illumination, and at sufficiently large values U under the influence of illumination, it is possible to tunnel nonequilibrium conduction electrons through a nanoscale organic coating, which increases the photocurrent. Due to low dark current the value k will slightly rise (in 2 times).

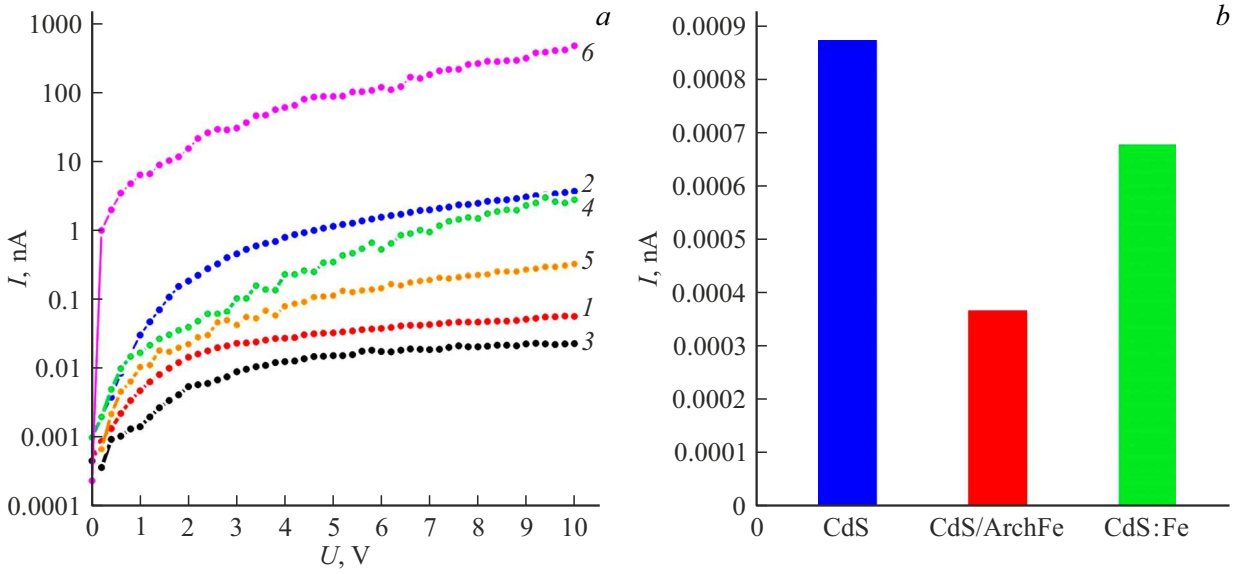

Figure 5. *a* — CVCs of CdS samples (curves *1*, *2*), CdS/ArchFe (curves *3*, *4*) and CdS:Fe (curves *5*, *6*), measured in darkness (*1*, *3*, *5*) and under illumination (*2*, *4*, *6*); *b* — values of dark currents I_{darc} measured at voltage of 0.2 V on samples CdS, CdS/ArchFe and CdS:Fe.

Table 2. Values of parameter k — ratio of the photocurrent at illumination of 20 000 lx to the value of dark current at fixed voltage U for each of the studied structures

Voltage		Values k	
U, V	CdS	CdS/ArchFe	CdS:Fe
3	20	12	720
10	60	122	1460

The effect of increasing the multiplicity of current variation under illumination in heterophase materials and structures can be caused by various mechanisms, and has been observed previously for both organic [30], as well as for inorganic [31] and hybrid materials. For example, a similar effect was previously observed on heterophase materials CdS-PbS [27] and was explained by a decrease in the rate of recombination of nonequilibrium charge carriers due to the outflow of radiation and technological defects into nanoscale PbS inclusions. In this case, the change in CVCs sample under illumination after its doping with iron can be considered as an indirect prove of the previously established fact of FeS [17] nanoinclusions formation.

Conclusion

Thus, the LB technology was found promising for the formation of a heterophase structure CdS-FeS, the use of which made it possible to create a material with an extended range of properties, and not only to preserve, but also to increase the photosensitivity of the material tenfold.

LB technology is promising because of a fairly simple assessment of the surface concentration of metal atoms transferred to the surface of a semiconductor substrate. Varying the number of deposited monolayers made it possible to change the parameters of a limited iron source within the required limits, ensuring the formation of nanoinclusions of a ferromagnetic phase of a given size at a given depth. The size of FeS phase and its distribution across the depth were estimated through modelling of the parallelly run processes of Fe diffusion, formation and precipitation of FeS.

A study of CdS photosensitivity during formation of a nanostructured material CdS-FeS showed a significant increase in photocurrents and a decrease in dark currents, which led to a rise of photosensitivity by 20–40 times. The observed effect fits within the framework of the theory describing electronic processes in heterophase semiconductors under the influence of irradiation [31]. Since in our study the observed effect occurs only after formation of nanoscale precipitates in a previously homogeneous material, it is logical to associate it with one of the types of photochemical reactions - the release of mobile donors (Cd ions) from the nanoscale phases of FeS solid solutions as a result of reducing potential inter-phase barriers during illumination. As the authors [32] emphasized, this type of photochemical reactions generally results in sensitization of „major“ semiconductor(CdS, in our case). In addition, in the dark, the narrow-band FeS inclusions serve as getters of mobile defects and electronic excitations [31], and provide higher dark resistance of the material and

also higher multiplicity of changes in the resistance of the semiconductor when illuminated.

Funding

The study was supported financially by the Russian Science Foundation — grant №22-22-00194, https://rscf.ru/project/22-22-00194/.

Conflict of interest

The authors declare that they have no conflict of interest.

References

[1] J. Cibert, D. Scalbert. Spin Phys. Semicond., **157**, 389 (2008), DOI: 10.1007/978-3-540-78820-1_13
[2] W. Zaleszczyk, E. Janik, A. Presz, P. Dłuzewski, S. Kret, W. Szuszkiewicz, J.F. Morhange, E. Dynowska, H. Kirmse, W. Neumann, A. Petroutchik, L.T. Baczewski, G. Karczewski, T. Wojtowicz. Nano Lett., **8** (11), 4061 (2008). DOI: 10.1021/nl802449g
[3] F. Matsukura, H. Ohno. *Nanomagnetism and Spintronics*, ed. Teruya Shinjo (Elsevier, Nanomagnetism and Spintronics, **277**, 2009), DOI: 10.1016/B978-0-444-53114-8.00007-8
[4] W. Dobrowolski, J. Kossut, T. Story. Handbook Magn. Mater., **15**, 289 (2003). DOI: 10.1016/S1567-2719(03)15003-2
[5] A. Bukhtiar, B. Zou. Mater. Adv., **5** (17), 6739 (2024). DOI: 10.1039/D4MA00523F
[6] D. Li, X. Zhang, W. He, Y. Peng, G. Xiang. Sci. China Mater., **67**, 279 (2024). DOI: 10.1007/s40843-023-2657-2
[7] J. Li, X. Zhang, J. Lu, W. He, Y. Nie, Y. Peng, G. Xiang. Nanoscale, **15** (5), 2206 (2023). DOI: 10.1039/D2NR05244J
[8] Y. Fan. J. Phys.: Conf. Series, **2608**, 012046 (2023). DOI: 10.1088/1742-6596/2608/1/012046
[9] R. Khan, I. Shigidi, S. Al Otaibi, K. Althubeiti, S.S. Abdullaev, N. Rahman, M. Sohail, A. Khan, S. Iqbal, T. Del Rosso, Q. Zaman, A. Khan. RSC Adv., **12** (55), 36126 (2022). DOI: 10.1039/D2RA06637H
[10] F. Pan, C. Song, X.J. Liu, Y.C. Yang, F. Zeng. Mater. Sci. Eng.: R: Reports, **62** (1), 1 (2008). DOI: 10.1016/j.mser.2008.04.002
[11] B. Sharma, R. Lalwani, R. Das. Optik, **281**, 170831 (2023). DOI: 10.1016/j.ijleo.2023.170831
[12] P. Li, C. Zhang, J. Lian, S. Gao, X. Wang. Solid State Commun., **151** (22), 1712 (2011). DOI: 10.1016/j.ssc.2011.07.042
[13] S.V. Stetsyura, P.G. Kharitonova. St. Petersburg State Polytechnical Univer. J. Phys. Mathem., **16** (1.2), 236 (2023). DOI: 10.18721/JPM.161.236
[14] L.A. Hernández, F.Martín, E. Berrios, G. Riveros, D.M. González, E. González, S. Lizama, F. Hernández. Arabian J. Chem., **13** (12), 8758 (2020). DOI: 10.1016/j.arabjc.2020.10.006
[15] Y. Li, S. Chen, K. Zhang, S. Gu, J. Cao, Y. Xia, C. Yang, W. Sun, Z. Zhou. New J. Chem., **44** (34), 1144 (2020). DOI: 10.1039/D0NJ01424A
[16] K. Kaur, G.S. Lotey, N.K. Verma. J. Mater. Sci.: Mater. Electron., **25** (6), 2605 (2014). DOI: 10.1007/s10854-014-1918-y
[17] S.V. Stetsyura, P.G. Kharitonova, I.V. Malyar. Appl. Phys., **5**, 66 (2020).
[18] S. Chandramohan, A. Kanjilal, S.N. Sarangi, S. Majumder, R. Sathyamoorthy, T. Som. Appl. Phys. A, **99** (4), 837 (2010). DOI: 10.1007/s00339-010-5598-z
[19] H.R. Dizaji, M. Ghasemian, M.H. Ehsani. Surf. Rev. Lett., **19** (2), 1250012 (2012). DOI: 10.1142/S0218625X12500126
[20] J.H. Al-Zahrani, M. El-Hagary, A. El-Taher. Mater. Sci. Semicond. Processing, **39**, 74 (2015). DOI: 10.1016/j.mssp.2015.04.042
[21] B. Lohitha, S. Thanikaikarasan, S. Roji Marjorie. Mater. Today: Proceedings, **33** (7), 3068 (2020). DOI: 10.1016/j.matpr.2020.03.513
[22] Z.K. Heiba, A.M. El-naggar, M.B. Mohamed, A.M. Kamal, M.M. Osman, A.A. Albassam, G. Lakshminarayana. Optical Mater., **122**, 111788 (2021). DOI: 10.1016/j.optmat.2021.111788
[23] N. Badera, B. Godbole, S.B. Srivastava, P.N. Vishwakarma, L.S. Sharath Chandra, D. Jain, M. Gangrade, T. Shripathi, V.G. Sathe, V. Ganesan. Appl. Surf. Sci., **254** (21), 7042 (2008). DOI: 10.1016/j.apsusc.2008.05.218
[24] S.V. Stetsyura, P.G. Kharitonova, E.G. Glukhovskoy. St. Petersburg State Polytechnical Univer. J. Phys. Mathemat., **15** (3.3), 250 (2022). DOI: 10.18721/JPM.153.349
[25] S.V. Stetsyura, E.G. Glukhovskoy, A.V. Kozlowski, I.V. Malyar. Tech. Phys., **60** (5), 746 (2015). DOI: 10.1134/S1063784215050266
[26] A. Mycielski. J. Appl. Phys., **63** (8), 3279 (1988). DOI: 10.1063/1.340813
[27] A.G. Rokakh. Pis'ma v ZhTF, **10** (13), 820 (1984) (in Russian).
[28] S.V. Bulyarskii, V.V. Svetukhin, O.V. Prikhod'ko. Semiconductors, **33** (11), 1157 (1999). DOI: 10.1134/1.1187839
[29] S.V. Stetsyura, I.V. Malyar, A.A. Serdobintsev, S.A. Klimova. Semiconductors, **43** (8), 1064 (2009). DOI: 10.1134/S1063782609080193
[30] S.G. Yudin, V.V. Bodnarchuk, V.V. Lazarev, A.I. Smirnova, S.V. Yablonskii. Liquid Crystals and their Application, **19** (4), 50 (2019). DOI: 10.18083/LCAppl.2019.4.50
[31] A.G. Rokakh, S.V. Stetsyura. Inorganic Mater., **33** (2), 153 (1997).
[32] M.K. Sheinkman, N.E. Korsunskaya. *Fotokhimicheskiye reaktsii v poluprovodnikakh tipa A2B6*. V kn. Fizika soyedineniy A2B6, ed. by A.N. Georgobiani, M.K. Sheinkman (Nauka, M., 1986)

Translated by T.Zorina